Desalination and Water Treatment
www.deswater.com
1944-3994/1944-3986 © 2012 Desalination Publications. All rights reserved
doi: 10/5004/dwt.2012.2909

Taylor & Francis
Taylor & Francis Group

44 (2012) 92–99
June

Aromatic compounds photodegradation catalyzed by ZnS and CdS nanoparticles

H.R. Pouretedal[a,*], H. Motamedi[b], A. Amiri[b]

[a]*Faculty of Science, Malek-Ashtar University of Technology, Shahin-Shahr, I.R. Iran*
Tel. +98 312 591 2253; Fax: +98 312 522 0420; email: HR_POURETEDAL@mut-es.ac.ir
[b]*Islamic Azad University, Shahreza branch, Shahreza, I.R. Iran*

Received 9 April 2011; Accepted 21 November 2011

ABSTRACT

The photodegradation of aromatic compounds such as nitrobenzene (NB), phenol, 2-nitrophenol (2-NP), 3-nitrophenol (3-NP), 4-nitrophenol (4-NP), 4-chlorophenol (4-CP), 2,4-dichlorophenol (2,4-DCP) and 2,4,6-trichlorophenol (2,4,6-TCP) are catalyzed by nanoparticles of zinc and cadmium sulfides. The photocatalytic degradation is studied in aqueous samples. The results show the highest degradation in pH of 11. The optimum dosages of catalysts obtained 0.3 and 0.5 g l^{-1} in degradation of NB and other aromatic compounds, respectively. The degradation kinetic of pollutants follows pseudo-first-order kinetic. The CdS semiconductor with band-gap 2.42 eV in comparison to ZnS with band-gap 3.54 eV indicates a higher photoactivity. The studies show the degradation rate of aromatic compounds in this order: NB > phenol, 2-NP > 4-NP > 3-NP > phenol and 2,4,6-TCP > 2,4-DCP > 4-CP > phenol. A reduction 90% in COD value and increasing 91% in TOC removal are obtained after photo-degradation of a sample contains all of aromatic compounds at duration time of 24 h.

Keywords: Photodegradation; Aromatic; Nanoparticle; ZnS; CdS

1. Introduction

Phenol and its derivatives such as CPs and NPs are industrially important chemicals and thus their presence in the environment is relatively very common [1]. Due to their high toxicity, they represent a group of dangerous chemicals even at low concentrations. Phenol and its derivatives are the precursors or intermediates in many process industries, such as dyes, resin and plastics, pharmaceutics, and pulp and paper. They are used as disinfectants, explosives, herbicides, and pesticides. They are irritants at low levels and affect the respiratory system and the central nervous system and can induce cancer at higher doses [2,3]. NB, also, is considered to be a highly toxic aromatic compound which is widely used in explosives, pesticides, prepharmo, and dye production and so on. The strong electron deficient character of its nitro-group results in NB resistant to oxidation by biological treatment and conventional chemical oxidation [4–6].

Voluminous literature is available on the photocatalytic degradation of NB , CPs, NPs, exploring the effect of number of substitutents and their positions, light intensity, temperature, pH, and influence of anions [7–14]. The photocatalytic degradation of NB and substituted NBs under UV exposure was investigated with combustion synthesized nano-TiO_2 and commercial TiO_2 catalyst, Degussa P-25 by Priya and Madras [12]. The photocatalytic degradation rates were considerably higher when catalyzed with combustion synthesized TiO_2 compared to that of Degussa P-25. Photo-degradation of CPs in the aqueous solution was reviewed by Czaplicka [15]. The review presents the CPs photo-degradation kinetics

*Corresponding author.

and mechanism in the aquatic environment under UV–Vis in the presence of hydroxyl radicals and singlet oxygen. Ahmed and co-workers reviewed the heterogeneous photocatalytic degradation of phenols in wastewater [16]. They showed that different parameters, such as type of photocatalyst and composition, light intensity, initial substrate concentration, amount of catalyst, pH of the reaction medium, ionic components in water, solvent types, oxidizing agents/electron acceptors, mode of catalyst application, and calcination temperatures can play an important role on the photocatalytic degradation of phenolic compounds in wastewater. Pathways of phenol and benzene photooxidation using TiO_2 supported on a zeolite was studied by Chen and co-workers [17]. The effect of the position of the Cl in DCPs and TCPs on the photodegradation kinetic was studied by D'Oliveira et al. [18].

The use of nanocrystalline semiconductors as photocatalysts, to initiate interfacial redox reactions, have generated great interest, due to their unique physicochemical properties, caused by their nanosized dimensions and large surface/volume ratios [19,20].

In this article, the photocatalytic degradation kinetic of NB, phenol, 2-NP, 3-NP, 4-NP, 4-CP, 2,4-DCP and 2,4,6-TCP are studied at the presence of ZnS and CdS nanoparticles as photocatalyst [21–25]. The sample conditions, structural factors of pollutants and nature of catalyst are discussed on the kinetic rate constants.

2. Experimental

2.1. Catalysts preparation

The ZnS and CdS nanoparticles were prepared by using controlled precipitation method [21–25]. The $Zn(CH_3COO)_2{\cdot}2H_2O$, $Cd(CH_3COO)_2{\cdot}2H_2O$, $Na_2S{\cdot}9H_2O$ and $HOCH_2CH_2SH$ (all from Merck) are used to synthesis the nanoparticles. Double distilled water is used to prepare solutions. To prepare the nanoparticles of ZnS and CdS, 50 ml of 0.1 M sodium sulfide solution in a decanter vessel is added drop by drop into 50 ml of 0.1 M of Zn^{2+} and/or Cd^{2+} ions and 0.5 M of 2-mercaptoethanol solution while the mixture was stirred vigorously at room temperature. The ZnS and/or CdS nanoparticles were separated, washed with deionized water and ethanol several times and dried in an oven at 80°C for 4 h.

The XRD patterns of nanoparticles and estimation of particles size were recorded by a Diffractometer Bruker D8ADVANCE Germany with Cu anode (λ = 1.5406 Å) and Ni filter. BET (Brunauer–Emmett–Teller) surface area of nanoparticles was determined by using Monosorb Quantochorom.

2.2. Photocatalytic degradation of aromatic compounds

The aqueous solutions (100 mg l^{-1}) of NB , phenol, 2-NP, 3-NP and 4-NP, 4-CP, 2,4-DCP and 2,4,6-TCP (all from Merck) were prepared as stock samples. Also, the diluted samples were prepared from stock samples. The aromatic degradation was carried out in a Pyrex photoreactor contain a high pressure mercury lamp 70 W with maximum irradiation at wavelength of 332 nm. The degradation was performed at suitable time intervals at room temperature while the samples were stirred continuously. The photoreactor was filled with 50 ml of 10–60 mg l^{-1} of aromatic compounds and 100–800 mg l^{-1} of ZnS and/or CdS catalyst.

The photocatalytic activity of nanosized ZnS and CdS also was studied by determination of the photonic efficiency of aromatic compounds photodegradation in aqueous suspension.

The irradiated samples were collected at regular intervals for analysis. The heterogeneous catalysts in samples were filtered through Millipore membrane filters and removed by using centrifuge prior to the analysis.

2.3. Sample analysis

The analysis of aromatic compounds samples was carried out by a UV–Vis spectrophotometer Carry-100 using a paired 1.0 cm quartz cell. The samples absorbance was recorded at λ_{max} of aromatic compounds in amplitude 300–400 nm before and after degradation. The degradation efficiency (%D) was calculated from initial concentration and residual concentration of aromatic compounds by spectrophotometric method.

The high-performance liquid chromatography (HPLC) method, also, was used to study degradation of aromatic compounds. HPLC chromatograms of aromatic compounds in degradation time intervals were obtained by using HPLC model HP with column of C18 and mixture of water:acetonitril (50:50) as mobile phase. The UV detector was used to record the chromatograms. The mineralization of aromatic molecules was followed by measurement of COD and TOC by using dichromate reflux and persulfate oxidation methods, respectively.

3. Results and discussion

3.1. Photodegradation of aromatic compounds

The photodegradation efficiencies of aromatic compounds catalyzed by ZnS and CdS nanoparticles are shown in Fig. 1. The conditions were 10 mg l^{-1} of aromatic compounds, 100 mg l^{-1} of nanocatalyst and pH 7. The XRD patterns of ZnS and CdS nanoparticles show the cubic structure for nanoparticles with average size of 8.6 and 10.3 nm, respectively. The surface area of nanoparticles from BET results is obtained 261 and 287 $m^2\ g^{-1}$ for ZnS and CdS, respectively. As seen from Fig. 1, the degradation efficiencies of aromatic compounds are increased with addition ZnS and/or CdS nanoparticles as photocatalyst. The photocatalytic activity of a

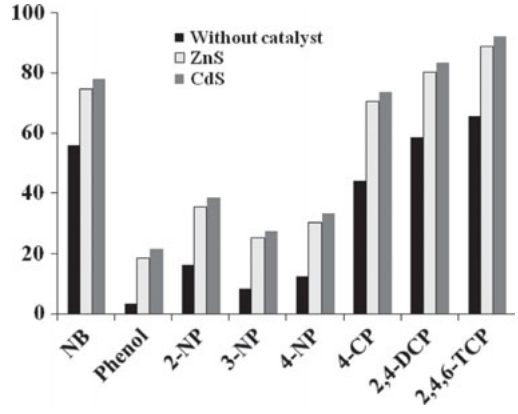

Fig. 1. Photo-degradation efficiency of aromatic compounds catalyzed by ZnS and CdS nanoparticles at pH 7 and irradiation time of 3 h.

semiconductor depends on surface and structural properties such as crystal composition, surface area, particle size distribution, porosity, band gap and surface hydroxyl density. The band-gap energies of ZnS and CdS semiconductors are 3.54 and 2.42 eV at 300 K, respectively [26,27]. Thus, the higher degradation efficiencies obtained at the presence of CdS with the lower band-gap energy.

Photocatalysis over a semiconductor such as ZnS and/or CdS is initiated by the absorption of a photon with energy equal to, or greater than the band gap of the semiconductor producing electron-hole (e^-/h^+) pairs. Consequently, following irradiation, the semiconductor particle can act as either an electron donor or acceptor for molecules in the surrounding medium. The electron and hole can recombine, releasing the absorbed light energy as heat, with no chemical effect. Otherwise, the charges can move to "trap" sites at slightly lower energies. The charges can still recombine, or they participate in redox reactions with adsorbed species. The valence band hole is strongly oxidizing, and the conduction band electron is strongly reducing. At the external surface, the excited electron and the hole can take part in redox reactions with adsorbed species such as water, hydroxide ion (OH^-), organic compounds, or oxygen. The charges can react directly with adsorbed pollutants, but reactions with water are far more likely since the water molecules are far more populous than contaminant molecules. Oxidation of water or OH^- by the hole produces the hydroxyl radical ($^\bullet OH$), an extremely powerful and indiscriminant oxidant. For a comparison, the oxidation potential of hydroxyl radical ($^\bullet OH$) is 2.8 V relative to the normal hydrogen electrode; cf. other substances used for water disinfection: ozone (2.07 V), H_2O_2 (1.78 V), HOCl (1.49 V) and chlorine (1.36 V). Hydroxyl radicals rapidly attack pollutants at the surface, and possibly in solution as well, and are usually the most important radicals formed in ZnS and/or CdS photocatalysis. An important reaction of the conduction band electron is reduction of adsorbed O_2 to $O_2^{\bullet}\downarrow$. This both prevents the electron from recombining with the hole and results in an accumulation of oxygen radical species that can also participate in attacking contaminants [27,28].

3.2. The effect of sample conditions

The pH of the samples dominates photodegradation process because many related properties such as the semiconductor's surface charge state, flat band potential, and dissociation of the pollutants are strongly pH dependence [29,30]. The effect of pH on the aromatic compounds photodegradation catalyzed by ZnS and CdS are shown in Figs. 2 and 3, respectively, in pH range of 3–12. The initial pH of samples was adjusted with

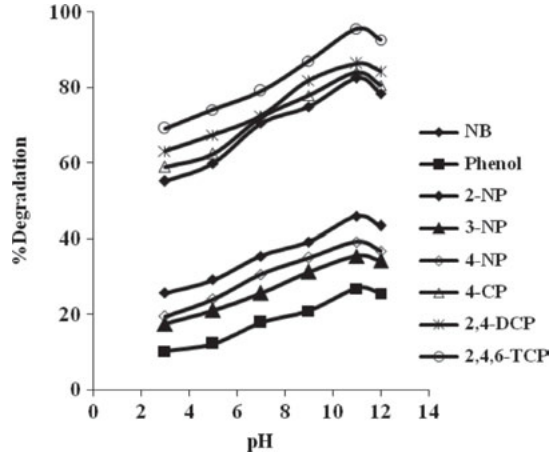

Fig. 2. The effect of initial pH of samples on the photodegradation of aromatic compounds catalyzed by ZnS nanoparticles (0.1 g l^{-1}).

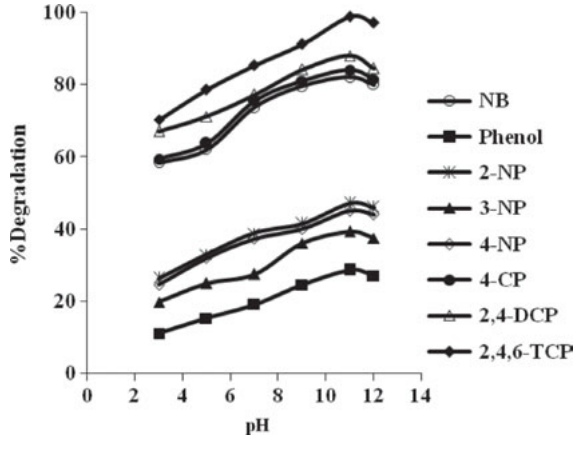

Fig. 3. The effect of initial pH of samples on the photodegradation of aromatic compounds catalyzed by CdS nanoparticles (0.1 g l^{-1}).

adding of suitable amounts of HCl and NaOH with concentrations of 1.0×10^{-1} M. The experiments were done at initial concentration 10 mg l^{-1} of aromatic compounds and 0.1 g l^{-1} of catalyst. As seen, the maximum degradation of aromatic compounds obtained at pH 11. The hydroxyl radicals will increase with increasing of the hydroxide ions (in upper pHs). Thus, the degradation will increase by increasing of the sample pH up to pH 11 but then decrease in upper pHs.

The point of zero charge (pHpzc) of ZnS and CdS is 7.0–7.5 [31] and is an important factor determining the distribution of the surface charge. Thus, the surface charge of ZnS and/or CdS is negative at pH > pHpzc, and is positive at pH < pHpzc. These characteristics affect significantly on the adsorption–desorption properties of ZnS and/or CdS surface. The pK_a of phenol is 9.95 and the pK_a values increase in NPs and CPs. Also, the charge of the phenols is dependent to pH of solution. When the pH is lower than the pK_a of the phenol derivatives, they are mainly present in neutrally molecular form. On the contrary, at pH greater than the pK_a they exist in the ionic form. Thus, the interaction and affinity vary between ZnS and CdS particles and phenols with solution pH. In pH ≤ 11, phenols are primarily present in the molecular form and the highest adsorption and degradation is obtained at these conditions. The higher pH of solution provide higher concentration of hydroxyl ions for reaction with the holes and formation hydroxyl radicals [6,7,21,22]. But, in pH > 11, the ionization of phenols occur and the phenolate ions are dominant in solutions. Therefore, the adsorption of phenol molecules on the surface of catalyst decrease because of the repulsive between the phenolat ions and catalyst particles.

Figs. 4 and 5 show the increasing of degradation with increasing the amounts of zinc sulfide and cadmium sulfide, respectively, up to 0.3 g l^{-1} for NB and 0.5 g l^{-1} for other aromatic compounds. Then, decreasing

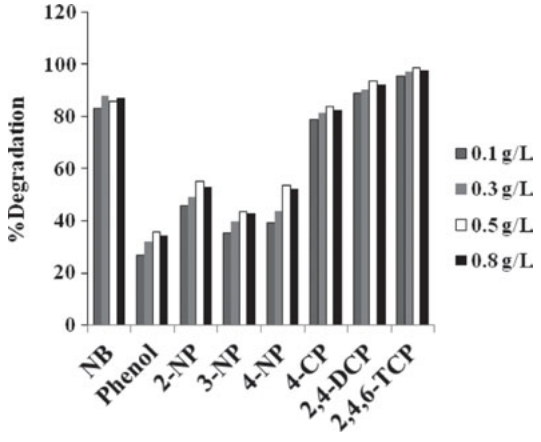

Fig. 4. The effect of ZnS dosage on the degradation efficiency of aromatic compounds at pH 11 and irradiation time of 3 h.

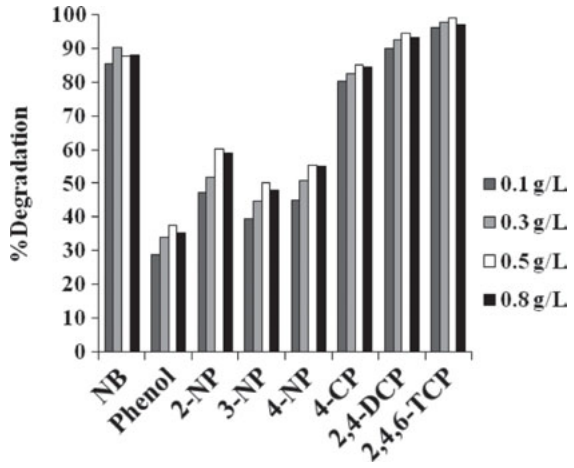

Fig. 5. The effect of CdS dosage on the degradation efficiency of aromatic compounds at pH 11 and irradiation time of 3 h.

of degradation is observed in upper of amounts of catalyst. The increasing of the degradation efficiency may due to the enhancement in the availability of active sites and thus the increasing of the number of aromatic molecules adsorbed on the surface of catalyst as well as the increasing the density of particles in the area of illumination. The degradation decreases at higher catalyst loading because the activated particles will be deactivated by agglomeration. Also, the radiation penetration is decreased and the radiation scattering is increased at higher amounts of catalyst [15–17,21–23]. Apparently, the ionization of phenolic compounds at pH 11 is due to the higher optimum dosage of catalysts in degradation of these pollutants in comparison to NB.

3.3. The photodegradation kinetic and structure of aromatic compounds

The kinetic model for heterogeneous photocatalysis is in accordance to the Langmuir–Hinshelwood kinetic expression ($\ln(C_o/C_t) = k_{obs}t$) [32]. The kinetic rate constants of aromatic compounds photodegradation catalyzed by ZnS and CdS nanoparticles are determined at initial concentrations 10, 20, 30, 40, 50, and 60 mg l^{-1} of pollutants at pH 11. The obtained k_{obs} values are shown in Tables 1 and 2 for ZnS and CdS catalysts, respectively. The maximum rate of degradation is obtained at initial concentration of 30 mg l^{-1} for NB. The increasing of kinetic rate constant up to 30 mg l^{-1} of NB is due to the increasing of the adsorption of NB molecules on the surface of catalyst. At higher concentrations, the decrease of active sites for hydroxyl radicals generation at the catalyst surface is due to decreasing of degradation rate. Also, increasing the adsorbed light by NB molecules and decreasing the photons number could reach the catalyst surface is one reason for decreasing of degradation rate at higher concentration

Table 1
The pseudo-first-order rate constants, k_{obs} (h^1), of photodegradation catalyzed by ZnS nanoparticles at different initial concentration (C_o) of aromatic compounds at pH 11

Aromatic compound	C_o, mg l^{-1}					
	10	20	30	40	50	60
NB	0.711	0.861	1.054	0.642	0.575	0.511
Phenol	0.152	0.128	0.109	0.097	0.088	0.082
2-NP	0.309	0.264	0.224	0.201	0.186	0.175
3-NP	0.174	0.149	0.135	0.124	0.112	0.100
4-NP	0.287	0.226	0.199	0.183	0.174	0.161
4-CP	0.948	0.811	0.647	0.524	0.512	0.472
2,4-DCP	1.213	0.894	0.753	0.698	0.642	0.555
2,4,6-TCP	1.417	1.004	0.812	0.571	0.467	0.415

Table 2
The pseudo-first-order rate constants, k_{obs} (h^1), of photodegradation catalyzed by CdS nanoparticles at different initial concentration (C_o) of aromatic compounds at pH 11

Aromatic compound	C_o, mg l^{-1}					
	10	20	30	40	50	60
NB	0.763	0.890	1.092	0.665	0.613	0.521
Phenol	0.183	0.151	0.129	0.11	0.098	0.090
2-NP	0.332	0.268	0.238	0.219	0.197	0.182
3-NP	0.189	0.173	0.161	0.152	0.136	0.118
4-NP	0.294	0.242	0.216	0.189	0.183	0.171
4-CP	0.974	0.867	0.703	0.633	0.581	0.532
2,4-DCP	1.286	1.055	0.888	0.764	0.657	0.601
2,4,6-TCP	1.554	1.067	0.823	0.705	0.575	0.471

[15,33]. The kinetic rate constants of phenolic compounds degradation are decreased with increasing of the initial concentration. The ionization of phenolic compounds at pH 11 is due to decreasing of adsorption of pollutant molecules on the surface of catalysts.

As seen from data of Tables 1 and 2, it can be concluded that the degradation rate is in this order: (1) NB > phenol, (2) 2-NP > 4-NP > 3-NP > phenol, and (3) 2,4,6-TCP > 2,4-DCP > 4-CP > phenol. The substitution of nitro group as an electron withdrawing in comparison to hydroxyl group as an electron donor is due to increasing of unstability of benzene ring. Thus, the higher degradation rate of NB in comparison to phenol is not surprising. The substitution of nitro group as an electron withdrawing in phenol is due to increasing of the aromatic ring activity to attack electrophilic hydroxyl radical. Thus, the reactivity of NPs is higher than that of phenol. The NPs were degraded by attachment of hydroxyl radical to the aromatic ring and formation of nitrocatechol or nitrohydroquinone is dominant in comparison to the formation of dihydroxy compounds by replacement of nitro group [34–36]. In benzene ring, the –OH and $–NO_2$ groups are an ortho- or para-directing group and a meta-directing group, respectively, that both groups influence the site of attacking hydroxyl radical. The substituted groups direct the hydroxyl radical to ortho- and para-position in 4-NP and 2-NP, respectively. The existence of two ortho-position versus one position is prominent in degradation of 2-NP versus 4-NP. For 3-NP, the hydroxy group dominates over the influence of nitro group in directing the radical to attack the para-position. Therefore, the degradation rate of NPs is obtained in this order: 2-NP > 4-NP > 3-NP [34–36].

The results indicate that the degradation rates of CPs are higher than phenol. Among the chlorinated phenols, the degradation rate increases with increasing chlorine substitution. The chlorine substitution is a group of electron enrichment and thus is suitable to attack hydroxyl radical. This is consistent with observations reported in the literature on the photodegradation of 2-CP, 2,4-DCP and 2,4,6-TCP in aqueous solution by the hydrogen peroxide aided reaction (hydroxyl radical provider) under UV irradiation [37].

In order to study the photocatalytic activity of ZnS and CdS nanoparticles, reaction rates are referred to the photonic efficiency. The photonic efficiency refers to the incident photon flux [38]. The initial photonic efficiencies were calculated as $\xi = r^0$ (mol l^{-1} s^{-1})/I^0 (Einstein l^{-1} s^{-1}), where r^0 is the initial reaction rate of aromatic degradation and I^0 is the incident photon flow per volumetric unit ($I^0 = 1.25 \times 10^{-6}$ Einstein l^{-1} s^{-1}) determined by UV-A radiometric measurements. The calculated values of ξ are on the wavelength of 332 nm (Table 3). The photonic efficiency results of ZnS and CdS photocatalysts

Table 3
Photonic efficiencies ($mol_{aromatic\ compounds}$ $Einstein^{-1}$) of the ZnS and CdS nanoparticles (0.5 g l^{-1}) photocatalysts at pH 11

Photocatalyst	Aromatic compound							
	NB	Phenol	2-NP	3-NP	4-NP	4-CP	2,4-DCP	2,4,6-TCP
ZnS	0.0087	0.0028	0.0041	0.0030	0.0035	0.0083	0.0074	0.0082
CdS	0.0109	0.0030	0.0042	0.0033	0.0039	0.0097	0.0085	0.0087

are in agreement with kinetic rate constants of aromatic compounds photodegradation.

The proposed mechanism for degradation of phenol and derivatives [35–37] is shown in Fig. 6. The results of degradation phenols such as CPs and NPs show the formation of intermediates during degradation process. The catechol, hydroquinone and pyrogallol are identified as intermediate products of degradation. The further photocatalytic oxidation of aromatic intermediates undergo to ring cleavage and formation of carboxylic acids and aldehydes. The CO_2 and H_2O are the final products of decorboxylation of carboxylic acids and aldehydes. The formation of organic acids such as muconic acid, fumaric acid, oxalic acid and formic acid duration of degradation is seen with a reduction of samples pH from 11 to 7–8. The chromatogram of samples before and duration of degradation show the formation of products with high polarity in comparison to phenol and its derivatives. So that, a reduction in retention times is observed with respect to C18 as stationary phase and H_2O:AN (50:50) as mobile phase.

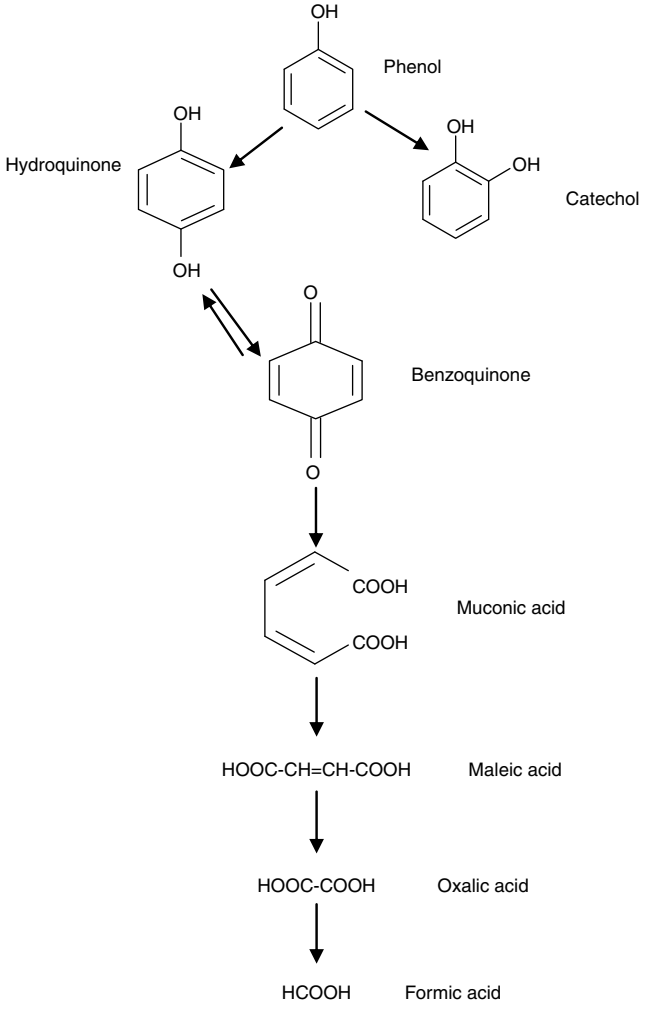

Fig. 6. The scheme of phenol degradation.

3.4. Mineralization tests

COD and TOC values have been related to the total concentration of organic materials in the solution and the decrease of COD and TOC reflects the degree of mineralization. The mineralization of all of aromatic compounds (NB, phenol, 2-NP, 3-NP-, 4-NP, 4-CP, 2,4-DCP and 2,4,6-TCP with concentration 10 mg l^{-1} of each pollutant) in photodegradation process catalyzed by ZnS and CdS nanoparticles was studied by using COD and TOC determination duration of 24 h. The ratio of COD/CODo and TOC removal percent at time intervals of 4 h versus time are shown in Figs. 7 and 8, respectively.

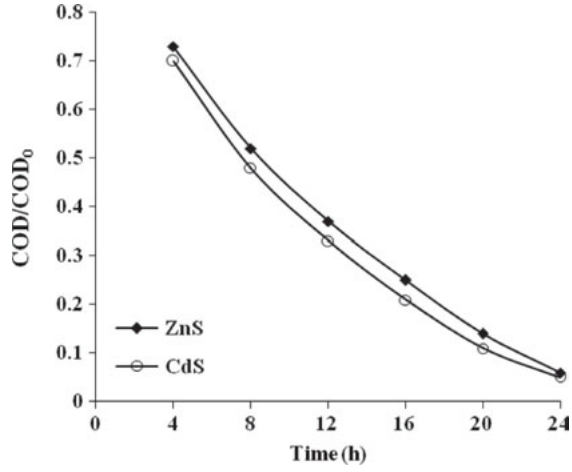

Fig. 7. The ratio of COD/CODo versus time of a sample contains all of aromatic compounds (10 $mg^{-1}l$ of each pollutant) in degradation process.

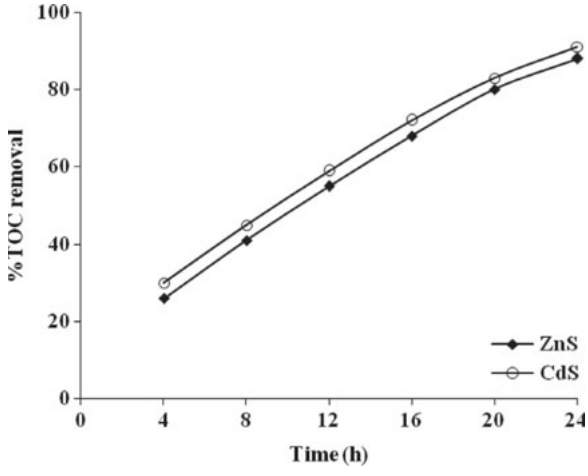

Fig. 8. The TOC removal percent versus time of a sample contains all of aromatic compounds (10 mg l^{-1} of each pollutant) in degradation process.

The reduction of COD values and increasing the %TOC removal show the degradation of aromatic compounds under irradiation. However, the COD value after 24 h indicates that there is still a residual amount of organic compounds, consisting of low mass molecules such as carboxylic acids in the treated solution [35,36].

4. Conclusions

Aromatic compounds such as benzene, phenolic compounds are well known for acute toxicity. These compounds are being introduced continuously into the aqueous waste through various anthropogenic inputs. Thus, the treatment of waste of aromatic compounds is a major impediment to the widespread acceptance of water recycling. The photodegradation of waste at presence of photocatalysts such as ZnS and/or CdS nanoparticles is an improvement in this area. The proposed method is a nonselective procedure so that the aromatic compounds NB, phenol, 2-NP, 3-NP, 4-NP, 4-CP, 2,4-DCP and 2,4,6-TCP in a sample are degraded more than 90% duration 24 h and the mineralization is confirmed by using HPLC chromatograms, COD and TOC analysis before and after degradation.

References

[1] M. Rodriguez, A. Kirchner, S. Contreras, E. Chamarro and S. Esplugas, Influence of H_2O_2 and Fe(III) in the photodegradation of nitrobenzene, J. Photochem. Photobiol. A, 133 (1–2) (2000) 123.
[2] D.S. Bhatkhande, V.G. Pangarkar and A.A.C.M. Beenackers, Photocatalytic degradation for environmental applications, J. Chem. Technol. Biotechnol., 77 (2001) 102–116.
[3] D.S. Bhatkhande, V.G. Pangarkar and A.A.C.M. Beenackers, Photocatalytic degradation of nitrobenzene using titanium dioxide and concentrated solar radiation: chemical effects and scaleup, Water Res., 37 (2003) 1223–1230.
[4] R. Dillert, M. Brandt, I. Fornefett, U. Siebers and D. Bahnemann, Photocatalytic degradation of trinitrotoluene and other nitroaromatic compounds, Chemosphere, 30 (1995) 2333–2341.
[5] Y. Mu, H.Q. Yu, J.C. Zheng, S.J. Zhang and G.P. Sheng, Reductive degradation of nitrobenzene in aqueous solution by zerovalent iron, Chemosphere, 54 (2004) 789–794.
[6] G. Sivalingam, M.H. Priya and G. Madras, Kinetics of the photodegradation of substituted phenols by solution combustion synthesized TiO_2, Appl. Catal. B, 51 (2004) 67–76.
[7] T. Pandiyan, O.M. Rivas, J.O. Martinez, G.B. Amezcua and M.A. Marinez-Carrillo, Comparison of methods for the photochemical degradation of chlorophenols, J. Photochem. Photobiol. A, 146 (2002) 149–155.
[8] M. Pera-Titus, V. Garcia-Molina, M.A. Banos, J. Gimenez and S. Esplugas, Degradation of chlorophenols by means of advanced oxidation processes: a general review, Appl. Catal. B, 47 (2004) 219–256.
[9] K. Nagaveni, G. Sivalingam, M.S. Hedge and G. Madras, Photocatalytic degradation of organic compounds over combustion synthesized Nano-TiO_2, J. Environ. Sci. Technol., 38 (2004) 1600–1604.
[10] M. Ksibi, A. Zemzemi and R. Boukchina, Photocatalytic degradability of substituted phenols over UV irradiated TiO_2, J. Photochem. Photobiol. A, 159 (2003) 61–70.
[11] J. Lea and A.A. Adesina, Oxidative degradation of 4-nitrophenol in UV-illuminated titania suspension, J. Chem. Technol. Biotechnol., 76 (2001) 803–810.
[12] M.H. Priya and G. Madras, Kinetics of photocatalytic degradation of chlorophenol, nitrophenol, and their mixtures, Ind. Eng. Chem. Res., 45 (2006) 482–486.
[13] C.H. Chiou, C.Y. Wu and R.S. Juang, Photocatalytic degradation of phenol and *m*-nitrophenol using irradiated TiO_2 in aqueous solutions, Sep. Purif. Technol., 62 (2008) 559–564.
[14] L.F. Liotta, M. Gruttadauria, G. Di Carlo, G. Perrini and V. Librando, Heterogeneous catalytic degradation of phenolic substrates: catalysts activity, J. Hazard. Mater., 162 (2009) 588–606.
[15] M. Czaplicka, Photo-degradation of chlorophenols in the aqueous solution, J. Hazard. Mater., B134 (2006) 45–59.
[16] S. Ahmed, M.G. Rasul, W.N. Martens, R. Brown and M.A. Hashib, Heterogeneous photocatalytic degradation of phenols in wastewater: a review on current status and developments, Desalination, 261 (2010) 3–18.
[17] J. Chen, L. Eberlein and C.H. Langford, Pathways of phenol and benzene photooxidation using TiO_2 supported on a zeolite, J. Photochem. Photobiol. A, 148 (2002) 183–189.
[18] J.C. D'Oliveira, C. Minero, E. Pelizzetti and P. Pichat, Photodegradation of dichlorophenols and trichlorophenols in TiO_2 aqueous suspensions: kinetic effects of the positions of the Cl atoms and identification of the intermediates, J. Photochem. Photobiol. A, 72 (1993) 261–267.
[19] D. Beydoun, R. Amal, G. Low and S. McEvoy, Role of nanoparticles in photocatalysis J. Nanopart. Res., 1 (1999) 439–458.
[20] P.V. Kamat and D. Meisel, Nanoparticles in advanced oxidation processes, Curr. Opin. Colloid Interface Sci., 7 (2002) 282–287.
[21] H.R. Pouretedal, A. Norozi, M.H. Keshavarz and A. Semnani, Nanoparticles of zinc sulfide doped with manganese, nickel and copper as nanophotocatalyst in the degradation of organic dyes, J. Hazard. Mater., 162 (2009) 674–681.
[22] H.R. Pouretedal, H. Eskandari, M.H. Keshavarz and A. Semnani, Photodegradation of organic dyes using nanoparticles of cadmium sulfide doped with manganese, nickel and copper as nanophotocatalyst, Acta Chim. Sinica., 56 (2009) 353–361.
[23] H.R. Pouretedal and M.H. Keshavarz, Synthesis and characterization of $Zn_{1-x}Cu_xS$ and $Zn_{1-x}Ni_xS$ nanoparticles and their applications as photocatalyst in Congo red degradation, J. Alloys. Compd., 501 (2010) 130–135.
[24] H.R. Pouretedal, M.H. Keshavarz, M.H. Yosefi, A. Shokrollahi and A. Zali, Photodegradation of HMX and RDX in the presence of nanocatalyst of zinc sulfide doped with copper, Iran. J. Chem. Chem. Eng., 28 (2009) 13–19.
[25] H.R. Pouretedal, M.H. Keshavarz, M.H. Yosefi, A. Shokrollahi and A. Zali, Photodegradation of HMX and RDX wastewater with CdS/Cu nanophotocatalyst, Chinese J. Energetic. Mater., 16 (2008) 745–752.
[26] A. Mills and S. LeHunte, An overview of semiconductor photocatalysis. J. Photochem. Photobiol. A, 108 (1997) 1–35.
[27] P. Kundu, P.A. Deshpande, G. Madras and N. Ravishankar, Nanoscale ZnO/CdS heterostructures with engineered interfaces for high photocatalytic activity under solar radiation. J. Mater. Chem., 21 (2011) 4209–4216.
[28] Q. Zhuo, H. Ma, B. Wang and F. Fan, Degradation of methylene blue: Optimization of operating condition through a statistical technique and environmental estimate of the treated wastewater, J. Hazard. Mater., 153 (2008) 44–51.
[29] K. Rajeshwar, M.E. Osugi, W. Chanmanee, C.R. Chenthamarakshan, M.V.B. Zanoni, P. Kajitvichyanukul and R. Krishnan-Ayer, Heterogeneous photocatalytic treatment of organic dyes in air and aqueous media, J. Photochem. Photobiol. C, 9 (2008) 171–192.
[30] M.S. Moignard, R.O. James and T.W. Healy, Adsorption of calcium at the zinc sulphide-water interface, Aust. J. Chem., 30 (1977) 733–740.
[31] H. Al-Ekabi and N. Serpone, Kinetic studies in heterogeneous photocatalysis, J. Phys. Chem., 92 (1988) 5726–5731.
[32] T. Aarthi, P. Narahari and G. Madras, Photocatalytic degradation of Azure and Sudan dyes using nano TiO_2, J. Hazard. Mater., 149 (2007) 725–734.

[33] M. Faisal, M. Abu Tariq and M. Muneer, Photocatalysed degradation of two selected dyes in UV-irradiated aqueous suspensions of titania, Dyes Pigment, 72 (2007) 233–239.
[34] M. Hugul, R. Apak and S. Demirci, Modeling the kinetics of UV/hydrogen peroxide oxidation of some mono-, di-, and trichlorophenols, J. Hazard. Mater., 77 (2000) 193–208.
[35] M.H. Priya and G. Madras, Photocatalytic degradation of nitrobenzenes with combustion synthesized nano-TiO_2, J. Photochem. Photobiol. A, 178 (2006) 1–7.
[36] G. Sivalingam, M.H. Priya and G. Madras, Kinetics of the photodegradation of substituted phenols by solution combustion synthesized TiO_2, Appl. Catal. B, 51 (2004) 67–76.
[37] S. Song, L. Xu, Z. He, H. Ying, J. Chen, X. Xiao and B. Yan, Photocatalytic degradation of C.I. Direct Red 23 in aqueous solutions under UV irradiation using $SrTiO_3/CeO_2$ composite as the catalyst, J. Hazard. Mater., 152 (2008) 1301–1308.
[38] J. Marugán, D. Hufschmidt, M. López-Munõz, V. Selzer and D. Bahnemann, Photonic efficiency for methanol photooxidation and hydroxyl radical generation on silica-supported TiO_2 photocatalysts, Appl. Catal. B, 62 (2006) 201–207.